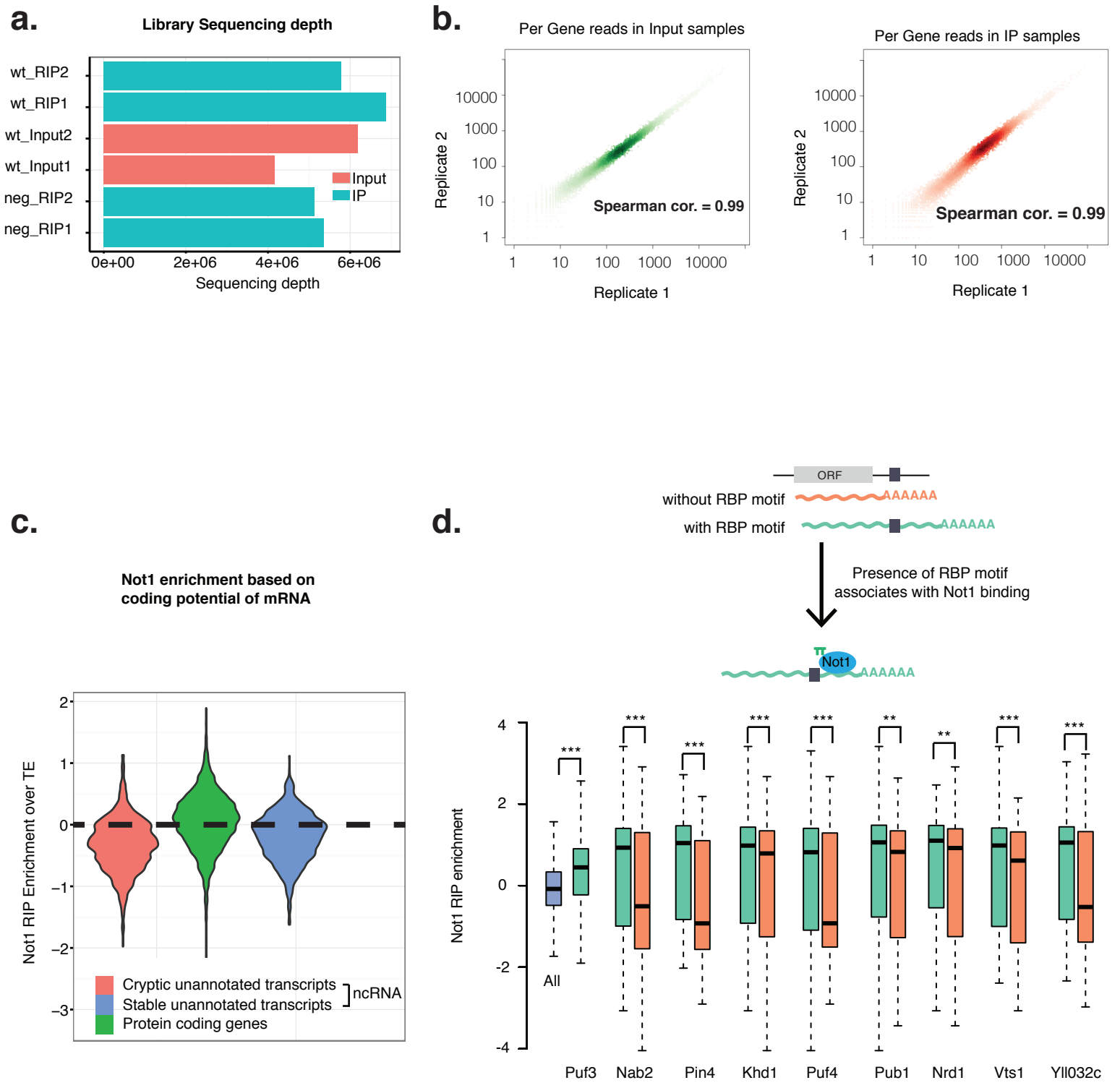

Figure S1. **Not1 RIPs, related to Figure 1**

a. Barplots for the number of aligned reads (in millions) for Input, negative and RIP samples from the Not1 RIP experiment for both the replicates. **b.** Scatter-plot between the number of reads aligned per gene between the replicates of input (green) and IP samples (red) from the biological replicates. Inset shows that Spearman correlation is greater than 0.98. **c.** Violin plots for Not1 RIP Log2 fold enrichment per gene for different categories of transcripts based on their coding potential shows that Not1 is enriched over coding mRNA (green) while it is depleted over non-coding mRNA (Cryptic annotated transcripts in red, and Stable unannotated transcripts in blue). **d.** Boxplots show the distribution of Not1 Log2 enrichment over the two different categories of polyadenylation isoforms belonging to genes with a particular predicted RBP binding motif (schematic on top). In the boxplots, all the polyadenylation isoforms are in blue, polyadenylation isoforms of genes which contain the predicted motif of the specified RBP (below) are in green while all the other polyadenylation isoforms of the same genes are in orange. Isoform specific association of Puf3 with mRNAs was as defined in (Gupta et al., 2014) and the other RBPs as in (Riordan et al., 2011). Comparison of the median Not1 binding between the two categories of polyadenylation isoforms (with RBP motifs and without RBP motif) by a student's t-test after multiple testing correction was performed and the more significant p-values were denoted by more number of stars. For several RBPs the p-values are highly significant hence these have two or more stars.

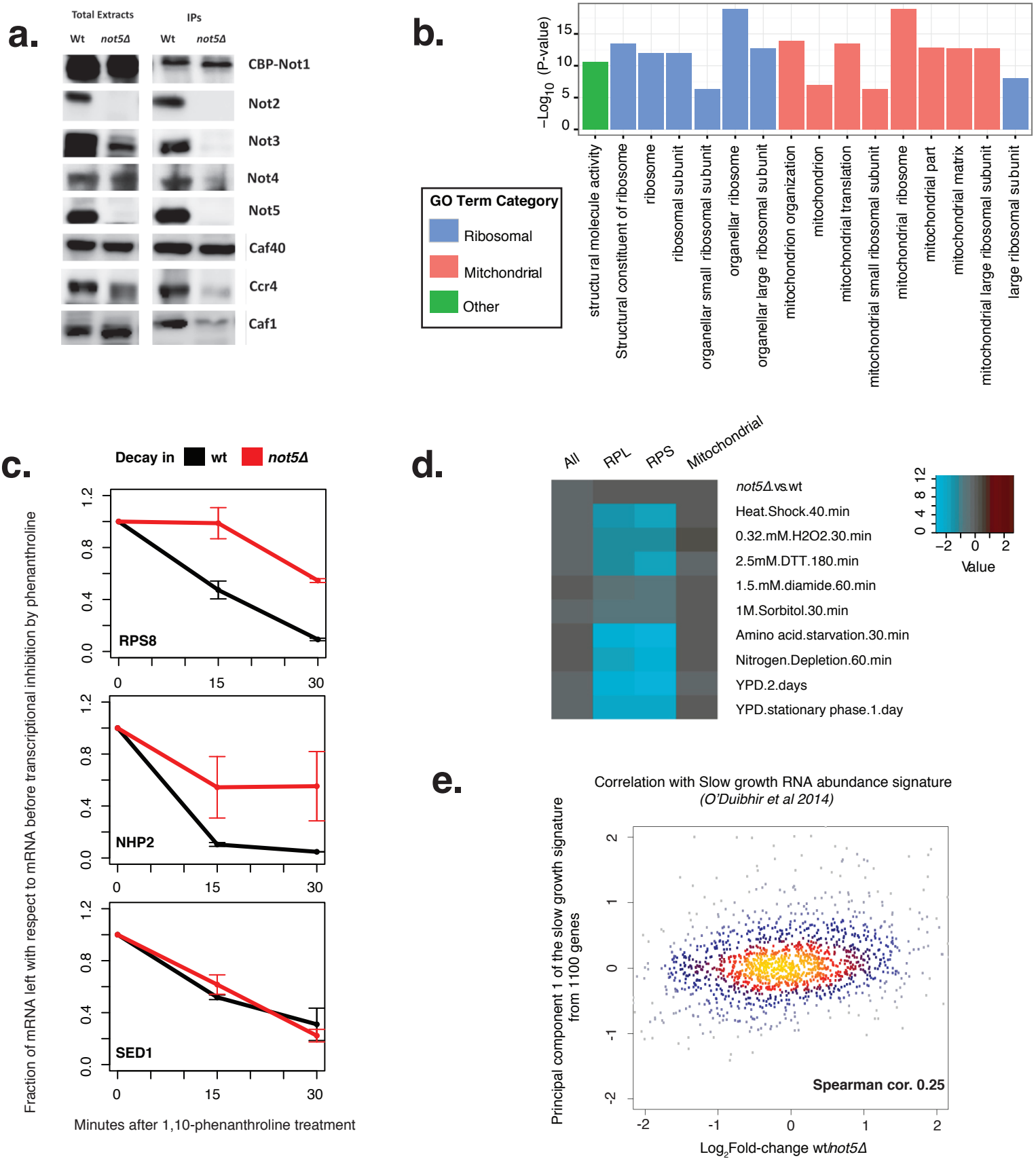

Figure S2. Loss of Not5 affects the composition and function of the Ccr4-Not complex, related to Figure 2

a. Levels of Ccr4-Not subunits in wild type and *not5*Δ cell extracts and in Not1-immunoprecipitates. We used TAP tagged Not1 expressing strains to purify Not1 by single affinity. We followed both the uncleaved and cleaved tagged Not1 in total extracts and in the immunopurifications with α-CBP antibody (Anti-Calmodulin Binding Protein; DAM1411288; Millipore). Other Ccr4-Not subunits were followed by specific polyclonal antibodies generated in our laboratory. **b.** Chart shows RIP binding probability in the absence of Not5 for the same category of gene ontologies that were enriched in Not1 RIPs done in wild type (Fig. 1c). **c.** Plots of mRNA levels of *RPS8, NHP2, SED1* versus time after 1,10-phenanthroline treatment to follow mRNA decay. As a loading control we measured 26S rRNA. Error bars representing SD. **d.** Heatmap of change in RNA abundance in different stress and slow growth conditions with respect to growth in glucose at permissive temperature from a previous study (Gasch et al., 2000) shows that RPL and RPS genes are repressed globally as compared to the mitochondrial genes. **e.** A scatter plot between the first component of the slow growth phenotype signature (O'Duibhir et al., 2014) and the Log_2 fold change in RNA abundance between wild-type and *not5*Δ background is only weakly correlated (Spearman correlation 0.25).

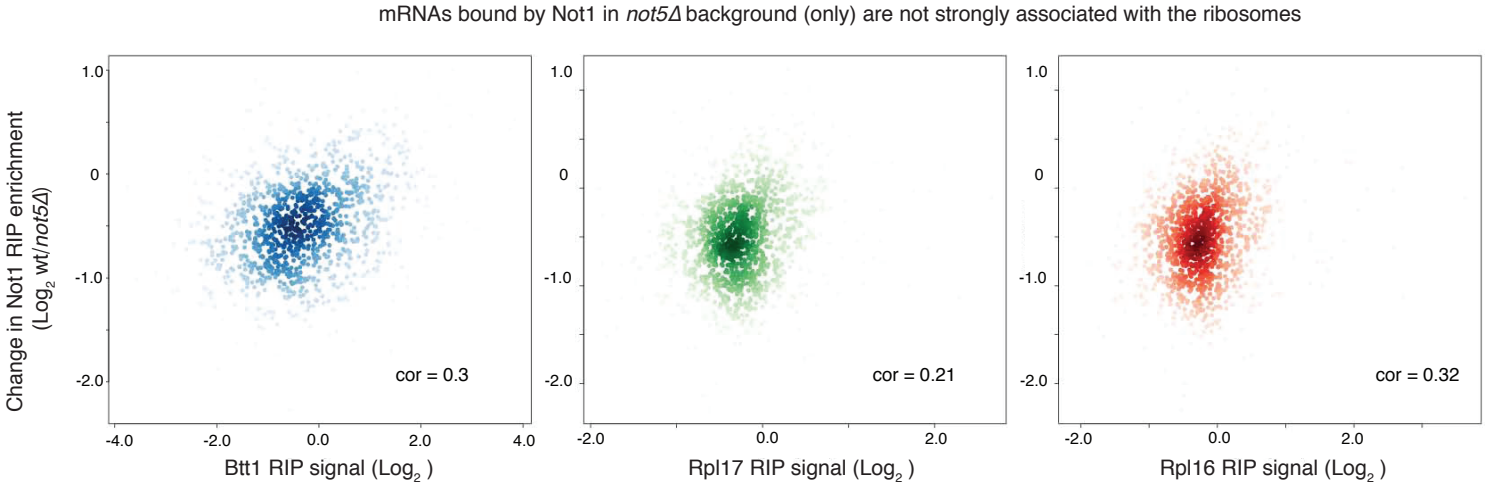

Figure S3. mRNAs bound by Not1 only in *not5*Δ do not correlate with translated mRNAs, related to Figure 3

Scatter plot between Log_2 fold change in Not1 RIP signal strength (wt/*not5*Δ) with Btt1, Rpl17 and Rpl16 RIP signal strength (del Alamo et al., 2011) for genes significantly enriched in Not1 RIP in *not5*Δ background only show weaker Spearman correlation (inset) than for genes in Fig 3.

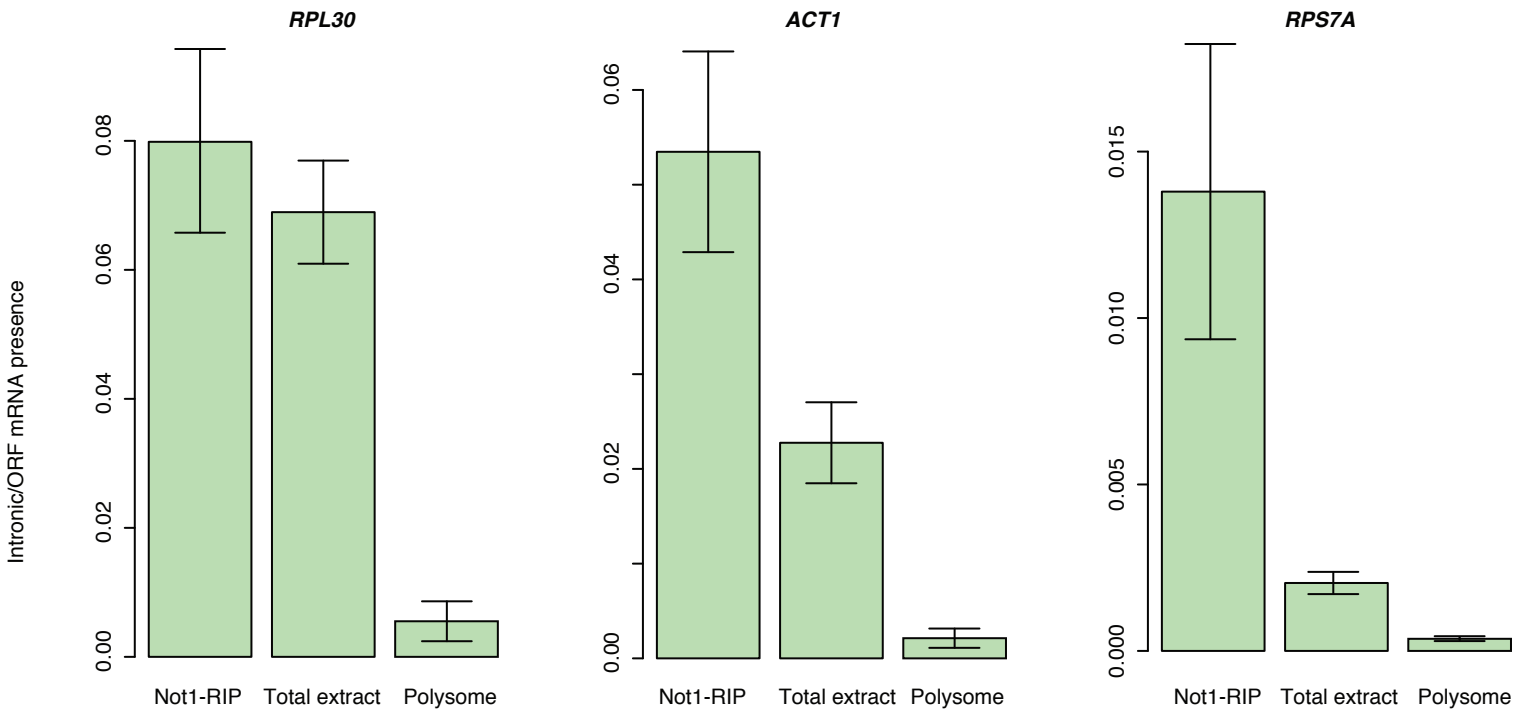

Figure S4. Not1 is bound to unspliced nuclear mRNAs, related to Figure 5

RPL30, ACT1 and *RPS7A* intron/ORF presence ratio in Not1 RIP, total extract and polysomes. The relative efficiency of intronic and ORF region specific primer pairs was evaluated using qPCRs done with a series of dilutions of known concentration genomic DNA. This determination was used for appropriate calculations of the relative presence of RNA sequences in Not1-RIP, total extract and polysomes. Error bars representing SD.

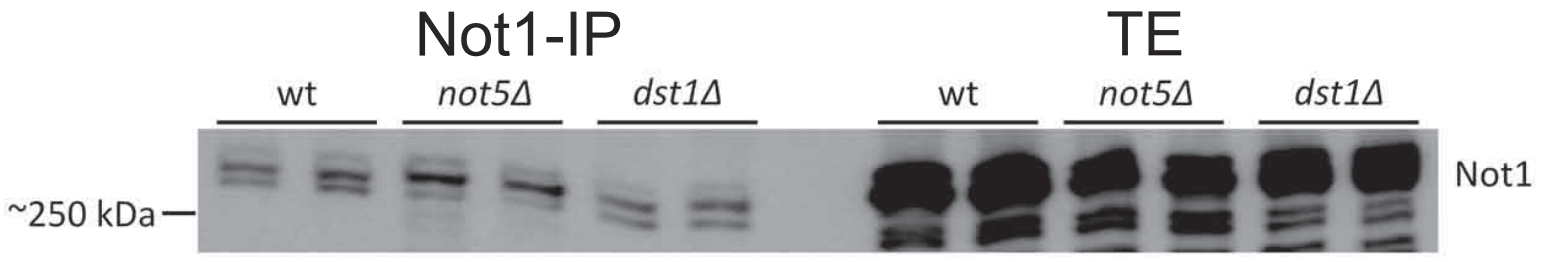

Figure S5. Not1 is immunoprecipitated similarly from wild type, *not5*Δ and *dst1*Δ cells, related to Figure 5e
Comparison of Not1 expression and immunoprecipitation from wild type, *not5*Δ and *dst1*Δ. Western-blot analysis was done as described in the legend of Figure S2a.

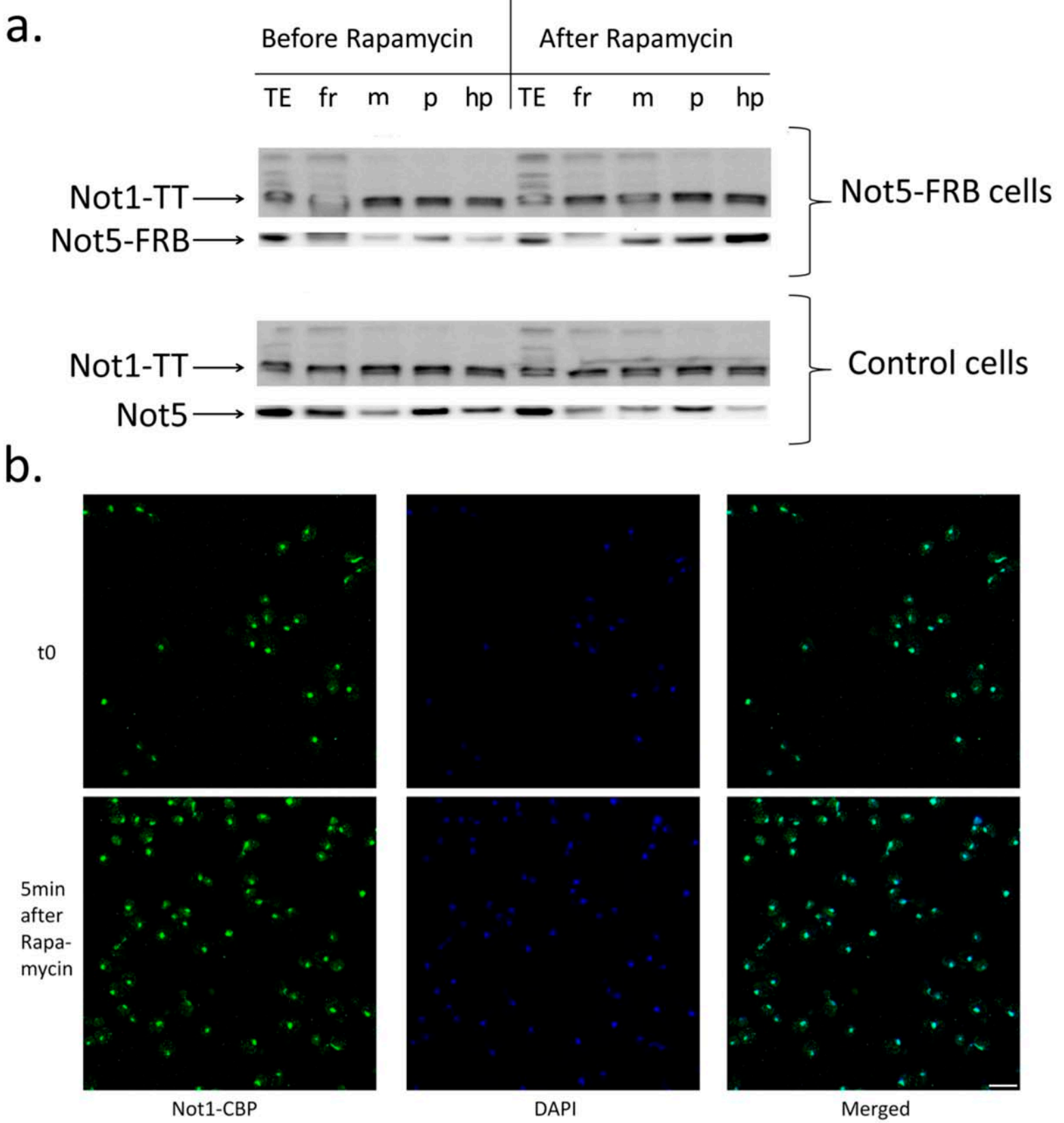

Figure S6. Not1 is not recruited to polysomes nor removed from the nucleus upon tethering of Not5-FRB to polysomes after rapamycin treatment, related to Figure 7

a. Not1 and Not5 distribution along the sucrose gradient before and after 5 minutes of rapamycin treatment in Not5-FRB expressing (upper panel) and in control (lower panel) cells. Lysates from yeast grown exponentially treated or not for 5 minutes with 1μg/ml of rapamycin were applied on a 12 ml 7–47% sucrose gradient. Fractions were separated by SDS-PAGE and analyzed by western blotting for Not5 using a polyclonal antibody that was generated in our laboratory and for Not1 using an anti-CBP antibody. Not1-TT: TAP tagged Not1 (Tap consists of the calmodulin binding peptide (CBP) followed by tobacco etch virus protease (TEV protease) cleavage site and Protein A) TE: total extract, fr: free fractions, m: monosome fractions, p: polysome fractions, hp: heavy polysome fractions. b. The localization of Not1-TT in Not5 tether away cells (MY11473 in Table S3) was evaluated by immunofluorescence before (t0) and after treatment for 5 minutes with rapamycin using an anti-CBP antibody. The nucleus is shown in blue (DAPI), Not1-TT is shown in green (Alexa-fluor) and the signals are merged in the right panels. Scale bar represents 10 μm.

SUPPLEMENTAL TABLES AND LEGENDS

Supplemental tables available as xls files:

Table S1. **RNA-IP from wt and *not5*Δ Not1 tap tagged strains, related to Figures 1 and 2**

Table S2. **Differentially enrichment of genes between wt and *not5*Δ polysomes, related to Figure 4**

Table S3. **SILAC data for wt and *not5*Δ strains with 3 hour heavy label growth, related to Figure 4**

qPCR primers used		
qPCR primer name	Type	Sequence
RPS8	Forward	5'-AATGCTACAGGACCTCTCTTT-3'
	Reverse	5'-AACTCGGCGTTTCATAAGAGG-3'
IMH1	Forward	5'-ACTGTAGGCAATGAGCTTGTGG-3'
	Reverse	5'-TTGGCTACCTTGTTCTGCGATG-3'
RPL30 ORF	Forward	5'-TCATCATTGCCGCTAACACTCC-3'
	Reverse	5'-TACCGACAGCAGTACCCAATTC-3'
RPL30 INTRONIC	Forward	5'-TGGGATTAGCAAGAAGGCTTGG-3'
	Reverse	5'-ATGGAGAAGCATCCTTTGAACG-3'
NHP2	Forward	5'-TGCCTGCTGTGTTGCCATTC-3'
	Reverse	5'-ACCTGGGACGATAAAGACAACTGAG-3'
RPB1	Forward	5'-GTCACCAAGTTACAGCCCAAC-3'
	Reverse	5'-AGATCCTGGGCTGTAGCCTG-3'
NIP1	Forward	5'-AGCTGATGAGCGTGCTAGAC-3'
	Reverse	5'-AGGAACGACGAATGGATTTTGGAG-3'
RPS22A	Forward	5'-ACCATCCTCCAAGGTCATTATCAAG-3'
	Reverse	5'-ATGGTCCATGATACCAGCAGAG-3'
RPS7A	Forward	5'-CGACGTTGCTGGTGGTAAGAAG-3'
	Reverse	5'-TGAACAGCAGTCAAGGTTCTGG-3'
RPS7A INTRONIC	Forward	5'-TTGGCTGACTATCGCCTGAAC-3'
	Reverse	5'-CATGGACGACACCGCTTAGAAC-3'
ACT1 ORF	Forward	5'-TTGTCCGTGACATCAAGGAA-3'
	Reverse	5'-ACCCAAAACAGAAGGATGGA-3'
ACT1 INTRONIC	Forward	5'-GCTTGCACCATCCCATTTAAC-3'
	Reverse	5'-CAGTCAATATAGGAGGTTATGGGAG-3'
MNN4	Forward	5'-CCCTTGGGATAACGATTTCGAC-3'
	Reverse	5'-TACCCTGTCTTGGGTCTTCC-3'
SED1	Forward	5'-TGAGCCAGAGGAAGTGGAGATG-3'
	Reverse	5'-TCCTATTATCTGCCGGTTTAGCCTC-3'
25S rRNA	Forward	5'-GAGTCGAGTTGTTTGGGAATGC-3'
	Reverse	5'-TGCCCTTCCCTTTCAACAATTTC-3'

Strains used		
Genotype	Strain name	Origine
MATa leu2Δ20 ura3Δ met15Δ lys2Δ his3Δ1	BY4741	Euroscarf
MATα leu2Δ20 ura3Δ met15Δ lys2Δ his3Δ1 not1:NOT1-Tap-URA3	MY4856	This study
MATα leu2Δ20 ura3Δ met15Δ lys2Δ his3Δ1 not1:NOT1-Tap-URA3 not5::NATMX4	MY5676	This study
MATa leu2Δ20 ura3Δ met15Δ lys2Δ his3Δ1 dst1::KANMX4 not1::NOT1-Tap-URA3	MY11990	This study
MATa tor1-1 fpr1::loxP-LEU2-loxP RPL13A-2×FKBP12::loxP	HHY221	A kind gift of Ulrich Laemmli
MATa tor1-1 fpr1::loxP-LEU2-loxP RPL13A-2×FKBP12::loxP not5::NOT5-FRB-HIS3MX4 not1::NOT1-Taptag-KanMX4	MY11473	This study
MATa tor1-1 fpr1::loxP-LEU2-loxP RPL13A-2×FKBP12::loxP not1::NOT1-Taptag-KanMX4	MY12195	This study

Table S4. List of strains and primers used in this study, related to Figures 5, 6 and 7

SUPPLEMENTAL REFERENCES

del Alamo, M., Hogan, D.J., Pechmann, S., Albanese, V., Brown, P.O., and Frydman, J. (2011). Defining the specificity of cotranslationally acting chaperones by systematic analysis of mRNAs associated with ribosome-nascent chain complexes. PLoS Biol *9*, e1001100.

Gasch, A.P., Spellman, P.T., Kao, C.M., Carmel-Harel, O., Eisen, M.B., Storz, G., Botstein, D., and Brown, P.O. (2000). Genomic expression programs in the response of yeast cells to environmental changes. Mol Biol Cell *11*, 4241-4257.

Gupta, I., Clauder-Munster, S., Klaus, B., Jarvelin, A.I., Aiyar, R.S., Benes, V., Wilkening, S., Huber, W., Pelechano, V., and Steinmetz, L.M. (2014). Alternative polyadenylation diversifies post-transcriptional regulation by selective RNA-protein interactions. Mol Syst Biol *10*, 719.

O'Duibhir, E., Lijnzaad, P., Benschop, J.J., Lenstra, T.L., van Leenen, D., Groot Koerkamp, M.J., Margaritis, T., Brok, M.O., Kemmeren, P., and Holstege, F.C. (2014). Cell cycle population effects in perturbation studies. Mol Syst Biol *10*, 732.

Riordan, D.P., Herschlag, D., and Brown, P.O. (2011). Identification of RNA recognition elements in the Saccharomyces cerevisiae transcriptome. Nucleic Acids Res *39*, 1501-1509.